

# Thinner, Smaller, Faster: IR Techniques To Probe the Functionality of Biological and Biomimetic Systems

Kenichi Ataka, Tilman Kottke, and Joachim Heberle\*

IR spectroscopy · monolayers · reaction mechanisms ·  
single-molecule studies · time-resolved spectroscopy

**N***ew techniques in vibrational spectroscopy are promising for the study of biological samples as they provide exquisite spatial and/or temporal resolution with the benefit of minimal perturbation of the system during observation. In this Minireview we showcase the power of modern infrared techniques when applied to biological and biomimetic systems. Examples will be presented on how conformational changes in peptides can be traced with femtosecond resolution and nanometer sensitivity by 2D IR spectroscopy, and how surface-enhanced infrared difference absorption spectroscopy can be used to monitor the effect of the membrane potential on a single proton-transfer step in an integral membrane protein. Vibrational spectra of monolayers of molecules at basically any interface can be recorded with sum-frequency generation, which is strictly surface-sensitive. Chemical images are recorded by applying scanning near-field infrared microscopy at lateral resolutions better than 50 nm.*

## 1. Introduction

Chemistry is the science of the composition, structure, properties, and reactions of matter. From a physical point of view, chemistry is based on electron affinity. Thus, knowledge of the electronic structure and the dynamics is of immediate relevance to our fundamental understanding of reactivity. State-of-the-art electron microscopy is capable of imaging the (probability of the) location of electrons, in other words, the orbitals.<sup>[1]</sup> The movement of electrons can nowadays be traced by attosecond ( $10^{-18}$  s) spectroscopy.<sup>[2]</sup> More recently, ultra-high spatio-temporal resolution in all four dimensions was

achieved by time-resolved electron<sup>[3]</sup> and X-ray diffraction.<sup>[4,5]</sup> However, the application of these fascinating methodologies to biological specimens is hampered by the fact that liquid water is required to form and maintain their structural and dynamical integrity. Moreover, fragile biological material is destroyed easily by the indispensable high energy of the radiation used.

Vibrational spectroscopy is one of the most promising biophysical techniques for probing biomaterial with high temporal resolution and spatial sensitivity. Because of the low energy of the radiation used, infrared spectroscopy is an essentially nonperturbing technique. Although the observation of living organisms on the atomic level is still in its infancy, many vibrational spectroscopic methods can be applied to model systems. Typically, such biomimetic systems represent segments of the organism under close-to-physiological conditions. This Minireview presents and discusses recent technological advances in the vibrational spectroscopy of proteins. We categorize these advances in a) techniques applied to the observation of thin layers down to the level of a monolayer and less, b) observations of small areas beyond the diffraction limit, and c) approaches that are sufficiently fast to trace elementary reaction steps (Figure 1). THz spectroscopy, which is another emerging technique in biospectroscopy,<sup>[6,7]</sup> is not reviewed here because of space limitations.

[\*] Dr. K. Ataka, Prof. Dr. J. Heberle  
Fachbereich Physik – Experimentelle Molekulare Biophysik  
Freie Universität Berlin  
Arnimallee 14, 14195 Berlin (Germany)  
Fax: (+49) 30-838-56510  
E-mail: joachim.heberle@fu-berlin.de  
Homepage: <http://www.physik.fu-berlin.de/einrichtungen/ag/ag-heberle/index.html>

Dr. T. Kottke  
Fakultät für Chemie – Biophysikalische Chemie  
Universität Bielefeld  
Universitätsstrasse 25, 33615 Bielefeld (Germany)

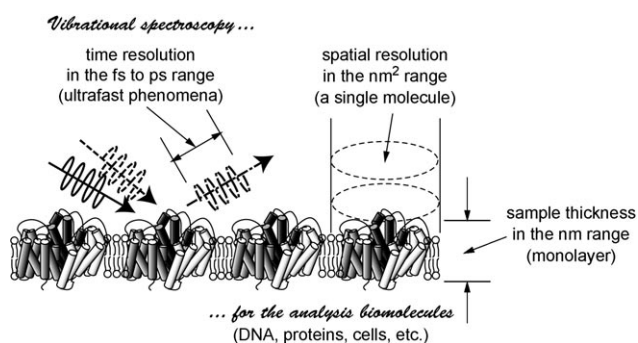


**Figure 1.** Sketch of the length and time scales of biological samples relevant to the vibrational techniques presented in this Minireview.

## 2. Thinner

The application of infrared spectroscopy to monolayers has a long history. It traces back to the 1960s to the development of the theory on infrared reflection absorption spectroscopy (IRRAS).<sup>[8]</sup> Experiments started with molecular studies on the solid/ultrahighvacuum (UHV) interface<sup>[9]</sup> but soon developed into studies on the solid (metal)/liquid<sup>[10–12]</sup> and air/liquid interfaces.<sup>[13]</sup> To probe the properties of the latter interface as a mimic of a cell membrane, lipid monolayers were studied extensively by IRRAS in combination with the Langmuir–Blodgett (LB) technique. This approach was extended to the analysis of the secondary structures of peptide and protein monolayers embedded in a lipid layer. Thakur and Leblanc investigated changes in the secondary structure and orientation of lysozyme in Langmuir monolayers in dependence of the surface pressure.<sup>[14]</sup> Kouzyzha et al. applied the same methodology to the alanine-rich polypeptide  $K_3A_{18}K_3$ .<sup>[15]</sup>

Although the improved sensitivity of IRRAS for the detection of monolayers on such surfaces is acknowledged, it is a great challenge to apply IR spectroscopy to functional studies of proteins on the monolayer level. The challenge behind the functional studies of enzymes is that minute structural changes must be detected in front of the bulk protein structure when the enzyme is catalytically active. The corresponding change in absorption can be as small as  $10^{-6}$ , and the sensitivity of IRRAS is usually not sufficient to detect

such small signals. In this case, the enhanced IR absorption employed in SEIRAS is superior.

### 2.1. Surface-Enhanced Infrared Absorption Spectroscopy (SEIRAS) of Monolayers

An alternative for monolayer detection by IR spectroscopy is the application of surface-enhanced infrared absorption (SEIRA) spectroscopy. SEIRA is a phenomenon where the IR absorption signal of a surface-bound molecule that is adsorbed on a nanoscale-roughened metal surface is enhanced (Figure 2a).<sup>[16]</sup> The enhancement is caused by a dielectric change of the metal film at the position of the molecular vibration. The broad absorption of the metal film, which is assisted by the surface plasmon polariton (SPP), covers the near-IR to the mid-IR region and is modulated by the dipole of the adsorbed molecules in a narrow vibrational range. The modulation occurs on the order of 10–100 fold of the original molecular vibration. As a consequence, the vibrational band of the adsorbed molecule is enhanced, although the real enhancement is caused by the change of the metal absorption itself. As with any optical near-field effect, signal enhancement in SEIRAS is restricted to the immediate vicinity of the surface and rapidly drops off within 10 nm. As a result the vibrational contributions of molecules on the surface can be discriminated from those in the bulk. Although SEIRAS can be performed in transmission configuration, it is advantageously exploited by using the attenuated total reflection (ATR) configuration, where a metal film with a thickness of about 10–100 nm is deposited on the reflection surface of the ATR prism. This optical configuration facilitates the manipulation of the sample conditions, for example, adsorption of sample on the metal film, exchange of the solution, illumination by light, and application of a voltage to the metal film.<sup>[17]</sup>

Since the field enhancement in SEIRA is restricted to the immediate vicinity of the surface, it is essential that the biological sample is tethered to the metal film. However, proteins are very susceptible to environmental conditions and may easily degrade when directly bound to the metal surface. Even when the protein is not completely denatured, it can malfunction when the binding conditions, for example, orientation, binding site, and distance from the metal surface,



Kenichi Ataka received his PhD in Chemistry from Tohoku University (1996, Sendai, Japan). As a postdoc (1996–2001), he worked with M. Osawa at the Catalytic Research Center at Hokkaido University (1996–2001, Sapporo). He moved to Germany in 2001 as a Alexander-von-Humboldt fellow and joined the group of J. Heberle first at the Research Center Jülich and later at Bielefeld University. He is currently at the Freie Universität Berlin as PREST fellow supported by the Japan Science and Technology Agency. His

research interests are applications of surface analytical techniques to functional studies of proteins and other biological molecules.



Tilman Kottke studied chemistry at Phillips-University Marburg, with a stay at Imperial College London. He received his PhD in Physical Chemistry at the University of Regensburg in 2003 for research with B. Dick. As a Helmholtz Young Investigator, he moved to Research Centre Jülich and later to Bielefeld University as a member of J. Heberle's group. He is currently working on his Habilitation in Bielefeld. His interests cover electronic and vibrational spectroscopies on biological blue-light receptors.

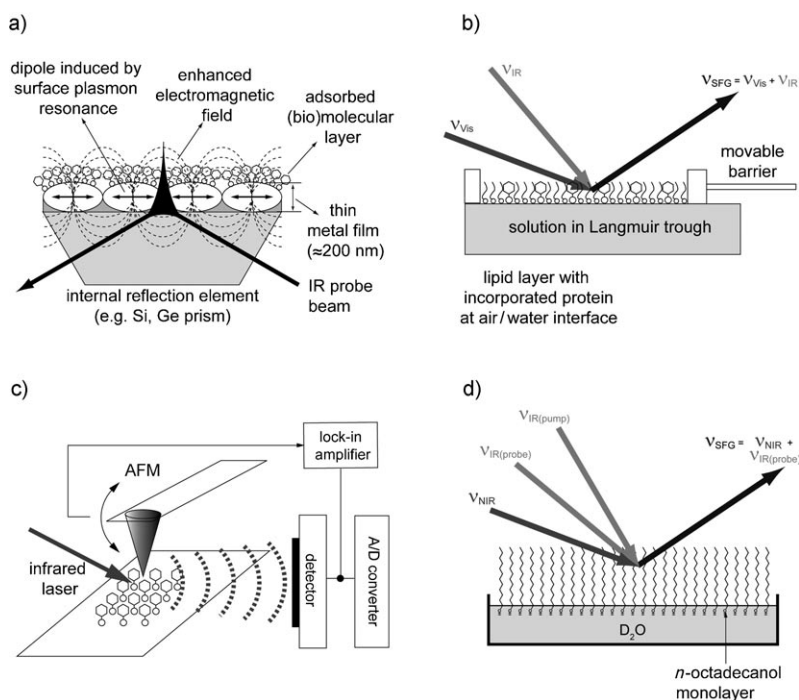


**Figure 2.** Experimental setups for a) SEIRAS, b) SFG, c) SNIM, and d) SFG-2D IR experiments.

are not properly chosen. Chemical modification of the solid surface is one of the practical solutions to control the adsorption conditions. The metal surface is “cushioned” by modification with a layer of organic molecules. This is achieved conveniently by the self-assembly of a monolayer (SAM) of thiol-terminated functional molecules. The key interaction is the strong affinity of the thiol group to the metal surface through quasi-covalent bonds.<sup>[18]</sup>

Since the field-enhancing metal film can be also employed as an electrode, SEIRAS has been often used for the investigation of electrochemical interfaces.<sup>[19,20]</sup> This is advantageous for the direct transfer of electrons to or from the adsorbed molecules, where SEIRAS monitors structural changes during the redox reaction (in situ). This approach was exploited for the first time in functional studies of redox-driven proteins: the structural changes of a cytochrome *c*

(cyt *c*) monolayer adsorbed on a Au electrode were monitored during redox cycling.<sup>[21,22]</sup> The surface of the gold electrode was chemically modified such that the bound cyt *c* was uniformly orientated; this enabled direct electron transfer through the external control of the electrode potential. Recording of the spectra was performed simultaneously with cyclic voltammetry, such that the direct correlation could be drawn between the structural changes of the protein (from FTIR difference spectroscopy) and the electron-transfer reaction (from electrochemistry). These experiments demonstrated that SEIDAS (surface-enhanced IR difference spectroscopy) captures the minute structural changes within cyt *c* during the redox reaction. The kinetics of the redox reaction were recorded in the micro- to millisecond regime by time-resolved SEIRAS measurements in combination with the potential jump transient recording method.<sup>[23]</sup>

The same strategy was applied in a functional studies on hydrogenases.<sup>[24]</sup> Wisitruangskul et al.<sup>[25]</sup> recorded SEIRA spectra of a [NiFe] hydrogenase, which reduces protons to generate  $H_2$ , during the redox reaction. SEIRAS was used to monitor the molecular structure of the CO and CN ligands at the binuclear Ni,Fe center of the hydrogenase during enzymatic production of hydrogen under potential control. Krassen et al.<sup>[26]</sup> studied a hybrid complex, which consisted of photosystem I from cyanobacteria and a hydrogenase on a solid gold surface, in situ by SEIRAS.<sup>[26]</sup> This hybrid complex demonstrated light-induced  $H_2$  evolution.

On account of the capacity of SEIDAS for monolayer detection, this technique is perfectly suited for functional studies on membrane proteins<sup>[27]</sup> which essentially exist as a monolayer in the native cell membrane. By proper orientational control through a chemically modified surface,<sup>[28,29]</sup> a



Joachim Heberle studied chemistry at the Universities of Stuttgart and Würzburg. He received a Diploma in Physical Chemistry from Würzburg University (1988), and a PhD in Biophysics from the Free University of Berlin (1991). After postdoctoral work at the Hahn-Meitner-Institute in Berlin, he headed an independent research group for Biomolecular Spectroscopy at the Research Centre Jülich (1993). He completed his Habilitation at Düsseldorf University in 1998 and was promoted to Full Professor in Biophysical Chemistry at Bielefeld University in 2005. Since 2009 he has been on the Faculty of Physics at the Freie Universität Berlin as a Full Professor in Experimental Molecular Biophysics.

biomimetic model system of a cell membrane can be produced on the surface of a metal electrode by which an electric field can be applied. The membrane potential is a key factor for the function of the membrane protein, but the effect of the potential on the protein function cannot be gauged by common structurally sensitive techniques. Jiang et al. applied this approach to study the photoreaction of sensory rhodopsin II,<sup>[30]</sup> one of two light sensors for the phototaxis of archaeobacteria. They demonstrated that the variation in electrode potential, equivalent to the change in membrane potential, exerts a specific effect on a single proton-transfer reaction but does not affect the structure. The developed technique holds promise not only for studies on the impact of the membrane potential on other membrane proteins but opens the way for studies on voltage-gated ion channels. This structurally sensitive method will be of utmost biomedical relevance.

The application of SEIRAS is not limited to the study of isolated proteins but has been extended to whole cells. Busalmen et al. measured adsorption and redox processes of the bacteria *Geobacter sulfurreducens* on a gold electrode surface by SEIRAS.<sup>[31,32]</sup> These Fe<sup>III</sup>-reducing bacteria support their growth by donating electrons to the metal in order to oxidize organic compounds. High numbers of *c*-type cytochromes are located in the outer membrane of the bacteria, such that electrons can be transferred by direct contact to the electrode. At the formal potential of 0.17 V (vs. Ag/AgCl), major changes in the SEIRAS spectra are similar to the spectrum of isolated cytochrome *c*.

## 2.2. Sum Frequency Generation (SFG)

A very powerful vibrational spectroscopic technique for the study of protein monolayers is sum frequency generation (SFG) spectroscopy (Figure 2b). SFG is a second-order nonlinear optical process in which two beams generate a third beam whose frequency is the sum of the optical frequencies of the two pump beams.<sup>[13]</sup> In SFG spectroscopy, two pulsed laser beams, typically one of fixed frequency in the visible range and one of tunable frequency in the infrared range, are overlapped spatially and temporally at an interface. Light at the sum frequency of both beams is collected in reflection. SFG is intrinsically surface-specific since it occurs only where the inversion symmetry is broken. This second-order nonlinear optical process is forbidden in media that possess inversion symmetry, for example bulk solution media. As a result, the specific SFG signal is detected exclusively from the monolayer at the interface without interference by background bulk signals.

The theory of SFG has been known since the 1960s, but received little attention.<sup>[33,34]</sup> SFG was rediscovered in the late 1980s as a surface analytical tool with submonolayer sensitivity.<sup>[35,36]</sup> To produce an SFG signal, intense laser pulses are required (e.g. 5–15  $\mu\text{J}$  per pulse,  $\Delta t = 3$  ps). In the early stages of SFG development, a major difficulty was the lack of tunable mid- and far-infrared sources with sufficient emission power, and investigations were limited to the near-infrared range of 3–5  $\mu\text{m}$  ( $> 2000$   $\text{cm}^{-1}$ ). Because of this restriction,

initial SFG studies on proteins and peptides focused mainly on C–H and O–H stretching vibrations,<sup>[37]</sup> which provided structural information about side-chain orientation (with the exception of a study using a free electron laser for the mid-IR range<sup>[38]</sup>). Only in the past five years have SFG studies been extended to the amide I region ( $\approx 1650$   $\text{cm}^{-1}$ ) owing to the development of high-power tabletop IR lasers.<sup>[39]</sup>

The main advantage of SFG spectroscopy is its versatile applicability to virtually any interface (solid/liquid, air/liquid, or liquid/liquid such as oil/water interfaces).<sup>[40]</sup> With this advantage SFG outperforms other surface-sensitive vibrational techniques such as SERS or SEIRAS, which are restricted to experiments on metal surfaces. The surface sensitivity of SFG has been further improved by the development of broadband heterodyne-detected SFG,<sup>[41]</sup> which can be used to monitor as low as a few percent of a monolayer. The application of SFG to biological samples was initially centered around structural studies of lipid layers at the air/water interface,<sup>[42]</sup> but was soon extended to studies of the secondary structures of membrane proteins embedded in lipid layers. Chen and co-workers were very active in using SFG as an in situ analytical tool to investigate the structure of small proteins (e.g. fibrinogen,<sup>[43,44]</sup> melittin,<sup>[45]</sup> and the foot protein of *Mytilus edulis*<sup>[46]</sup>) and membrane protein fragments (the  $\beta_{\text{V}}$  subunit ( $G_{\beta_{\text{V}}}$ ) of G-protein<sup>[47]</sup>) in lipid bilayers. As one example, they analyzed the amide I band to elucidate the binding and orientation of the  $G_{\beta_{\text{V}}}$  subunit in a POPC (1-palmitoyl-2-oleoyl-*sn*-glycero-3-phosphocholine) lipid bilayer.<sup>[47]</sup> As the amide I band reflects various secondary structural motifs of a complex protein structure, detailed structural analysis based on fitting the amide I band envelope is difficult. Introducing the polarization as an additional parameter and its variation in the pump and probe beams in SFG, for example SSP and PPP (denoting Vis/IR/SFG polarization, respectively), delivers additional structural parameters for band analysis. Based on such polarization-dependent data, the authors unambiguously determined the orientation of the  $G_{\beta_{\text{V}}}$  subunit to be tilted  $-35^\circ$  with respect to the surface normal of the lipid layer.

In conclusion, SFG represents a versatile method for the study of molecular processes at interfaces of any kind. However, the method is demanding because it requires state-of-the-art laser technology. The strength of SEIRAS lies in the ease of implementation and the possibility to study conformational changes and proton transfer in proteins during catalysis.

## 3. Smaller

### 3.1. Scanning Near-Field Infrared Microscopy (SNIM)

Although vibrational spectroscopy can probe structures down to the monolayer level (several nm), the lateral resolution is usually limited by diffraction (roughly 5  $\mu\text{m}$  for the mid-IR range). This limit was overcome by the invention of near-field proximal probes. The scanning near-field optical microscope (SNOM) reveals subwavelength detail, because it uses near-field probing rather than beam focusing.<sup>[48]</sup> SNOM

requires a fine aperture with a diameter substantially smaller than the wavelength. The light passing through such an aperture of diameter stays confined within a small distance behind the aperture, and it is in this region that the sample must be scanned to create a near-field image. Owing to the poor transmittance of the metallic aperture, the resolution is practically limited to  $\lambda/10$  ( $\approx 50$  nm). Extending this principle to the mid-infrared region leads to the unpleasant conclusion that the practical resolution is limited to about 1  $\mu\text{m}$ , which is often insufficient for imaging microscopy in the fields of subcellular biology or nanoelectronics. In so-called “scattering-type” scanning near-field infrared microscopy (s-SNIM),<sup>[49]</sup> enhanced spatial resolution is accomplished by the “apertureless” tip—a simple, sharp, metallic needle commonly used in atomic force microscopy (AFM; Figure 2c). This needle functions like an optical antenna and supplies a concentrated electric field at its apex. The high field at the tip has a transverse width which is about equal to the tip’s radius of curvature. Therefore, the microscope’s resolution is defined by the curvature (currently 10–20 nm<sup>[48]</sup>). The near-field interaction between the high field at the tip and sample is modulated by application of a small longitudinal oscillation to the tip. The modulated near-field signal is demodulated and amplified by the lock-in method to suppress background scattering signals. These tip manipulations are accomplished with a tapping-mode AFM with metal-coated cantilevers. Thus, the s-SNIM apparatus consists of a standard AFM combined with an IR-scattering measurement.

The first s-SNIM image was reported by Keilmann and Knoll.<sup>[49,50]</sup> They obtained a chemical image of a mixed layer of polymethylmethacrylate and polystyrene on a scale of about 100 nm, which is about one-hundredth of the applied wavelength ( $\lambda = 9\text{--}11$  nm from a CO laser). At the boundary of the two polymers, contrast changes were observed owing to changes in vibrational absorption. A strong enhancement of the contrast, in other words, the absorption signal, was observed, which suggests that SEIRA effects may occur at the optical near-field of the probe tip.

Kopf et al. recently reported s-SNIM experiments on SAM films of 1-octadecanethiolate and biotinylated alkylthiolate (BAT) formed on a gold substrate.<sup>[51]</sup> They clearly observed patterns of the two different SAMs with a lateral resolution of approximately  $90 \times 90$  nm<sup>2</sup>, which corresponds to the detection limit of 27 attogram ( $10^{-18}$  g) or about 30 000 BAT molecules. Although s-SNIM has not yet been applied to a monolayer or to the surface of biological samples, the technique looks promising for approaching the single-molecule detection limit of infrared spectroscopy without invasive labeling of the material.

SNIM may be compared to tip-enhanced Raman spectroscopy (TERS), which uses the same principle of scattering detection but employs visible laser sources.<sup>[52,53]</sup> This is an advantage over SNIM, where tunable mid-IR laser light must be used to achieve contrast. However, great care must be taken that the strong electromagnetic field present at the tip of the TERS setup does not damage the sensitive (biological) sample.

## 4. Faster

### 4.1. Time-Resolved Infrared Spectroscopy from Microseconds to Femtoseconds

Most of the crucial steps of enzyme catalysis proceed in the micro- to millisecond time domain. Conventional dispersive spectroscopy can be applied in this regime, but it is usually limited by the low flux of the available broadband IR light sources. Instead, tunable laser sources may be used as the probe, for example lead salt laser diodes.<sup>[54]</sup> The recent development of quantum cascade lasers in the mid-IR range might foster further development owing to their considerably higher power and ease of maintenance. A significant improvement in optical resolution and signal-to-noise ratio was achieved by using the step-scan approach developed in Fourier transform spectroscopy with its broadband (multiplex) detection.<sup>[55]</sup> The technique is commercially available as an option to state-of-the-art FTIR spectrometers; however, its application to complex systems that exhibit small difference signals still requires modifications by the user.<sup>[56]</sup> The step-scan approach was and is a valuable tool to investigate the mechanisms of many proteins, most of them light-gated. Recent examples cover the whole spectrum from the proton-pump bacteriorhodopsin<sup>[57]</sup> to blue-light sensors,<sup>[58,59]</sup> proteins from the light-harvesting complex,<sup>[60]</sup> and photosystem I.<sup>[61,62]</sup> The technique can even be applied to single, micrometer-sized crystals of proteins.<sup>[63]</sup>

Time-resolved spectroscopy on proteins with femtosecond time resolution is still challenging when conducted in the mid-IR range. The pump-probe approach is commonly accomplished in the visible spectral range, but the broad electronic bands are less informative than the detailed vibrational spectra when it comes to the details of a chemical reaction. Initially, single-wavelength measurements were performed, where the probe light of a continuous-wave IR laser was up-converted into the visible range for detection.<sup>[64]</sup> The employment of IR array detectors enabled the pump-and-probe approach with pulsed lasers to be applied, where the spectrally broad probe pulse was dispersed by a grating and the full spectral information was monitored at a specific delay time.<sup>[65]</sup> A further improvement came about by the introduction of stable all-solid-state titanium-sapphire lasers as sources for the pump and probe pulses. Difference signals in the infrared region are more than two orders of magnitude lower than in the visible as a result of the much lower extinction coefficient of IR absorption bands. Because of this and also the strong absorption of water in the mid-IR region, protein samples must be highly concentrated. Despite these challenges, the evolution of reactions from the excited-state surface were studied in several proteins with ultrafast dispersive infrared spectroscopy covering a broad spectral range. A special focus has been the isomerization reactions in photoreceptors; one of the fastest reactions in nature is the 200 fs switch of retinal in visual rhodopsin.<sup>[66]</sup> Using infrared spectroscopy, a time constant of 500 fs has been determined for the isomerization of retinal in the proton-pump bacteriorhodopsin.<sup>[67]</sup> More recent examples include the bistable switch of the linear tetrapyrrole in phytochromes, where light-

induced on-<sup>[68]</sup> and off-switching<sup>[69]</sup> has been followed for the first time by ultrafast IR spectroscopy. Another strength of infrared spectroscopy is the detection of hydrogen bonds. It has been shown that the breaking of a hydrogen bond plays a crucial role in the isomerization of the chromophore *p*-coumaric acid in photoactive yellow protein.<sup>[70]</sup> Similarly, a rearrangement of the hydrogen-bonding network surrounding the chromophore of the BLUF domain (a FAD-containing sensor of blue light) was postulated to take place in the primary step after electron transfer to the flavin cofactor.<sup>[71]</sup>

#### 4.2. Two-Dimensional IR Spectroscopy

A significant drawback of conventional (1D) IR spectroscopy of systems as complex as biomolecules is the lack of spatial information. For a molecular interpretation of the assigned signals in the framework of a reaction model, structural information derived from NMR spectroscopy or X-ray crystallography is necessary. In contrast, 2D IR spectroscopy provides spatial information independent of any other structural data by direct analysis of cross-peaks from vibrational couplings and comparison to theoretical models. It probes and resolves interactions between distant chemical functional groups. 2D IR spectroscopy is considered to be a complementary method to NMR spectroscopy, where the time resolution is limited to milliseconds, and to time-resolved X-ray crystallography.

2D IR spectroscopy in this context refers to fs-pulsed spectroscopy as opposed to conventional two-dimensional Fourier transform IR spectroscopy often referred to as correlation spectroscopy. The 2D IR experiment is performed either in the frequency domain<sup>[72]</sup> or in the time domain.<sup>[73]</sup> 2D IR spectroscopy in the frequency domain does not differ from conventional pump-probe spectroscopy and is achieved by scanning the narrow-band pump laser frequency and recording transient spectra with a broadband probe pulse at a defined time delay. The time-domain approach (echo spectroscopy) is similar in its pulse sequence to correlation spectroscopy (COSY) or nuclear Overhauser effect spectroscopy (NOESY) in NMR experiments.<sup>[74]</sup> A vibrational coherence is established, then interrupted, and the induced free induction decay (FID) is finally resolved over time. This relaxation is much faster than in NMR spectroscopy and leads to a time resolution of some tens of picoseconds in 2D IR experiments. In analogy to NMR spectroscopy, the Fourier transform of the FID then yields the 2D IR spectra.

Two main features arise in a 2D IR spectrum by comparison of measurements with and without a pump pulse. Pairs of diagonal elements are resolved that originate from the transitions of the excited oscillators. These signals reflect excited-state absorption (positive signal) and stimulated emission (negative signal). Additionally, ground-state absorption by the probe pulse after depopulation by the pump pulse contributes to the negative signal. The pair of signals is separated in frequency owing to anharmonicity (Figure 3). The second major feature is the occurrence of off-diagonal cross-peaks that are caused by inharmonic coupling between

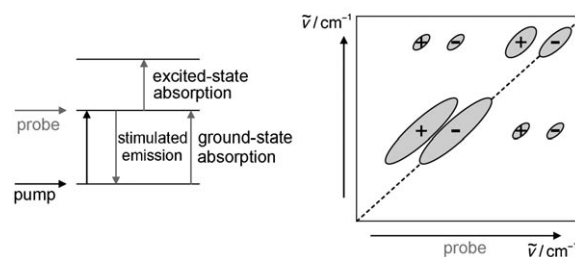


**Figure 3.** Schematic 2D IR spectrum showing negative contributions from stimulated emission and ground-state absorption and positive signals from excited-state absorption. Additional off-diagonal cross-peaks reveal vibrational couplings between oscillators and therefore contain information on the 3D structure.

different oscillators. They carry valuable information about the structure of the system.

One focus of 2D IR spectroscopy on complex molecules has been the amide I vibration of peptides and proteins. The C=O stretching vibration of the peptide backbone is a strong oscillator that couples to neighboring oscillators of similar frequency. These couplings can take place through space, for example through dipolar interactions, and through bonds (through the C<sub>α</sub> atoms of the peptide backbone or even across a hydrogen bond). Therefore, structural information is not directly derived from the couplings. Instead, the spectral patterns are analyzed with regard to angles and mutual orientation of the oscillators. In this procedure either a theoretical model is applied to simulate the spectra and to extract the information, or the different polarization dependence of the cross-peaks is used.<sup>[75]</sup> The capability of 2D IR and the validity of the models was first checked on the known structure of a cyclic pentapeptide.<sup>[76]</sup> In a next step, the coupling strength and the angle between the transition dipoles in tri-alanine with its two peptide carbonyls were determined.<sup>[77]</sup> From the coupling strength, the dihedral angles of the backbone were obtained with the help of quantum-chemical calculations. Thus, 3D structural parameters were retrieved from infrared spectroscopic experiments. To enable this breakthrough in the analysis of the weak cross-peaks, the strong diagonal peaks were suppressed by exploiting their different polarization dependence.<sup>[77,78]</sup> In the step to larger systems, this specific information is blurred by the large number of overlapping bands and the manifold of coupling mechanisms. However, it is possible to discriminate between different secondary-structure elements of peptides and proteins that are characterized by a specific position, splitting, amplitude, and line shape of the cross-peaks and diagonal peaks. This has been shown for antiparallel β-sheets of several model proteins<sup>[79]</sup> and 3<sub>10</sub>-α-helices of octapeptides.<sup>[80,81]</sup> A further improvement in specificity was achieved by analyzing the differences in coupling of the amide I' to the amide II' vibration.<sup>[82]</sup> 2D IR enables a refinement of the quantitative description of the exciton-like amide modes by theoretical models, which will have an impact on secondary-structure determination of proteins in general.

A major obstacle in the analysis of 2D IR spectra is spectral crowding. The overlap of signals can be overcome by introducing isotope labels in a site-specific manner to resolve

the contribution and environment of single residues. Through the  $^{13}\text{C}=\text{O}$ - and  $^{13}\text{C}=\text{O}$ -labeling of residues, coupling constants can be determined, for example within a helix.<sup>[83]</sup> This approach has been applied to a complete transmembrane (27 residues) domain of a human membrane protein by tracking inhomogeneous line-broadening to fluctuations in the different sections of the protein inside and outside of the membrane.<sup>[84]</sup> Isotopic labeling can also be used to remove couplings in very complex systems such as amyloid fibrils, which are found as plaques in brain tissue of patients with Alzheimer's disease.<sup>[85]</sup> Interstack distances within the fibrils were obtained from the coupling constants. The formation of amyloids by aggregation can be monitored directly by 2D IR spectroscopy; in this it is possible to access the kinetics of polypeptide aggregation with a residue-specific resolution and without external labeling.<sup>[86,87]</sup> In a very recent study on the M2 channel of the influenza virus, the empirical dependence of the line-shape of a series of isotopically labeled carbonyls from residues within the channel pore was used to derive structural information about rotational movements accompanying channel closure.<sup>[88]</sup> Remarkably, the membrane protein was studied in a near-native environment, which allowed a critical assessment of conflicting structures from solid-state NMR spectroscopy and X-ray crystallography. This development demonstrates that 2D IR spectroscopy, while being under development, is already capable of contributing to key biological questions.

The kinetics of ultrafast processes have been studied using 2D IR experiments. The main field of investigation has been protein folding. The high spatial sensitivity of IR spectroscopy in the sub-Ångström regime was exploited to detect the minute changes in hydrogen bonding accompanying folding processes. These changes are usually hidden in conventional 1D FTIR experiments because of spectral congestion. The additional dimension in the 2D experiment permits the comparison to molecular dynamics (MD) simulation. As an immediate result from such a combined theoretical and experimental approach, the speed limit of contact formation of protein side chains was revised from 20 ns in the original postulate<sup>[89]</sup> to 160 ps.<sup>[90]</sup> These results were obtained by monitoring changes in hydrogen-bonding strength in a small model peptide in which a  $\beta$  turn is restrained by a disulfide bond. The unfolding process was triggered by photolysis of the disulfide bond by a femtosecond UV light pulse. In an application to a larger system, the dynamics of the unfolding of ubiquitin was studied after a fast temperature jump.<sup>[91]</sup> The investigation of fast processes is not limited to amide modes: other strong oscillators such as CO gas may be exploited to trace enzyme kinetics. For example, the exchange of different substates in the CO binding of myoglobin was studied, where the cross-peaks indicate their interconnectivity.<sup>[92]</sup> The high time resolution of 2D IR was demonstrated by monitoring the exchange of the substrates on the 50 ps time scale.<sup>[93]</sup> Hamm and co-workers further demonstrated the feasibility of 2D IR difference experiments<sup>[94]</sup> by studying another work horse often employed in methodological development, the light-driven proton-pump bacteriorhodopsin. These authors were able to selectively analyze only those vibrations which

changed during the reaction. This very powerful trick extends the scope of this method to the whole vibrational spectrum.

Very promising is the combination of 2D IR with SFG (see Section 2.2). Similar to SEIRAS discussed above, 2D IR spectroscopy exploits the surface-selection rules to measure with monolayer sensitivity. A fourth near-IR pulse is introduced to the pulse sequence (sum frequency generation SFG 2D IR), which up-converts the radiated IR signal to the visible spectral region (Figure 2d).<sup>[95]</sup> Besides providing surface selectivity, the method makes it possible to determine the orientation of the aligned vibrational dipoles by an appropriate polarization of the laser pulses. So far this technique has been applied only to a dodecanol monolayer on water,<sup>[96]</sup> but it is a promising approach for experiments on more complex systems.

In summary, the strength of 2D IR spectroscopy is the combination of its sensitivity to structural elements with its high inherent time resolution. It does, however, not yet provide a direct measure of distances between structural elements. The number of distance restraints obtained is far less than in NMR spectroscopy. However, the analysis has yielded dihedral angles between functional groups in proteins which are valuable parameters in structure determination. Because of the high time resolution of 2D IR experiments, it is possible to investigate mechanisms, including the geometry of the transition state,<sup>[97]</sup> of processes in the picosecond time range not accessible by NMR spectroscopy.

*This work was supported by grants from the Deutsche Forschungsgemeinschaft (SFB 613, K8 and D11 to J.H., FOR 526 to J.H. and T.K.) and the PRESTO program of the Japan Science and Technology Agency (to K.A.).*

Received: December 17, 2009

Published online: June 16, 2010

- [1] J. M. Zuo, M. Kim, M. O'Keeffe, J. C. H. Spence, *Nature* **1999**, *401*, 49–52.
- [2] M. Hentschel, R. Kienberger, C. Spielmann, G. A. Reider, N. Milosevic, T. Brabec, P. Corkum, U. Heinzmann, M. Drescher, F. Krausz, *Nature* **2001**, *414*, 509–513.
- [3] A. Yurtsever, A. H. Zewail, *Science* **2009**, *326*, 708–712.
- [4] H. N. Chapman, S. P. Hau-Riege, M. J. Bogan, S. Bajt, A. Barty, S. Boutet, S. Marchesini, M. Frank, B. W. Woods, W. H. Benner, R. A. London, U. Rohner, A. Szoke, E. Spiller, T. Moller, C. Bostedt, D. A. Shapiro, M. Kuhlmann, R. Treusch, E. Plonjes, F. Burmeister, M. Bergh, C. Caleman, G. Hult, M. M. Seibert, J. Hajdu, *Nature* **2007**, *448*, 676–679.
- [5] A. Ravasio, D. Gauthier, F. R. Maia, M. Billon, J. P. Caumes, D. Garzella, M. Geleoc, O. Gobert, J. F. Hergott, A. M. Pena, H. Perez, B. Carre, E. Bourhis, J. Gierak, A. Madouri, D. Mailly, B. Schiedt, M. Fajardo, J. Gautier, P. Zeitoun, P. H. Bucksbaum, J. Hajdu, H. Merdji, *Phys. Rev. Lett.* **2009**, *103*, 028104.
- [6] U. Heugen, G. Schwaab, E. Brundermann, M. Heyden, X. Yu, D. M. Leitner, M. Havenith, *Proc. Natl. Acad. Sci. USA* **2006**, *103*, 12301–12306.
- [7] D. F. Plusquellic, K. Siegrist, E. J. Heilweil, O. Esenturk, *ChemPhysChem* **2007**, *8*, 2412–2431.
- [8] R. G. Greenler, *J. Chem. Phys.* **1966**, *44*, 310–315.
- [9] W. Suetaka, J. T. Yates, *Surface Infrared and Raman Spectroscopy, Methods and Applications*, Plenum Press, New York, **1995**.

- [10] A. Bewick, K. Kunimatsu, J. W. Russell, C. Gibilaro, M. Razaq, *J. Electrochem. Soc.* **1982**, *129*, C139.
- [11] A. Bewick, J. W. Russell, *J. Electroanal. Chem.* **1982**, *132*, 329–344.
- [12] J. W. Russell, J. Overend, K. Scanlon, M. Severson, A. Bewick, *J. Phys. Chem.* **1982**, *86*, 3066–3068.
- [13] Y. R. Shen, *Nature* **1989**, *337*, 519–525.
- [14] G. Thakur, R. M. Leblanc, *Langmuir* **2009**, *25*, 2842–2849.
- [15] A. Kouzayha, M. N. Nasir, R. Buchet, O. Wattraint, C. Sarazin, F. Besson, *J. Phys. Chem. B* **2009**, *113*, 7012–7019.
- [16] M. Osawa in *Handbook of Vibrational Spectroscopy, Vol. 1* (Eds: J. M. Chalmers, P. R. Griffiths), Wiley, Chichester, **2002**, pp. 785–799.
- [17] K. Ataka, J. Heberle, *Anal. Bioanal. Chem.* **2007**, *388*, 47–54.
- [18] J. C. Love, L. A. Estroff, J. K. Kriebel, R. G. Nuzzo, G. M. Whitesides, *Chem. Rev.* **2005**, *105*, 1103–1169.
- [19] G. Samjeske, A. Miki, M. Osawa, *J. Phys. Chem. C* **2007**, *111*, 15074–15083.
- [20] A. Yamakata, T. Uchida, J. Kubota, M. Osawa, *J. Phys. Chem. B* **2006**, *110*, 6423–6427.
- [21] K. Ataka, J. Heberle, *J. Am. Chem. Soc.* **2003**, *125*, 4986–4987.
- [22] K. Ataka, J. Heberle, *J. Am. Chem. Soc.* **2004**, *126*, 9445–9457.
- [23] N. Wisitruangsakul, I. Zebger, K. H. Ly, D. H. Murgida, S. Ekgasit, P. Hildebrandt, *Phys. Chem. Chem. Phys.* **2008**, *10*, 5276–5286.
- [24] H. Krassen, S. Stripp, G. von Abendroth, K. Ataka, T. Happe, J. Heberle, *J. Biotechnol.* **2009**, *142*, 3–9.
- [25] N. Wisitruangsakul, O. Lenz, M. Ludwig, B. Friedrich, F. Lenzian, P. Hildebrandt, I. Zebger, *Angew. Chem.* **2009**, *121*, 621–623; *Angew. Chem. Int. Ed.* **2009**, *48*, 611–613.
- [26] H. Krassen, A. Schwarze, B. Friedrich, K. Ataka, O. Lenz, J. Heberle, *ACS Nano* **2009**, *3*, 4055–4061.
- [27] K. Ataka, F. Giess, W. Knoll, R. Naumann, S. Haber-Pohlmeier, B. Richter, J. Heberle, *J. Am. Chem. Soc.* **2004**, *126*, 16199–16206.
- [28] K. Ataka, B. Richter, J. Heberle, *J. Phys. Chem. B* **2006**, *110*, 9339–9347.
- [29] X. Jiang, A. Zuber, J. Heberle, K. Ataka, *Phys. Chem. Chem. Phys.* **2008**, *10*, 6381–6387.
- [30] X. Jiang, E. Zaitseva, M. Schmidt, F. Siebert, M. Engelhard, R. Schlesinger, K. Ataka, R. Vogel, J. Heberle, *Proc. Natl. Acad. Sci. USA* **2008**, *105*, 12113–12117.
- [31] J. P. Busalmen, A. Esteve-Nunez, A. Berna, J. M. Feliu, *Angew. Chem.* **2008**, *120*, 4952–4955; *Angew. Chem. Int. Ed.* **2008**, *47*, 4874–4877.
- [32] J. P. Busalmen, A. Berna, J. M. Feliu, *Langmuir* **2007**, *23*, 6459–6466.
- [33] N. Bloembergen, R. K. Chang, S. S. Jha, C. H. Lee, *Phys. Rev.* **1968**, *174*, 813–822.
- [34] C. C. Wang, *Phys. Rev.* **1969**, *178*, 1457–1460.
- [35] X. D. Zhu, H. Suhr, Y. R. Shen, *Phys. Rev. B* **1987**, *35*, 3047–3050.
- [36] J. H. Hunt, P. Guyotsionnest, Y. R. Shen, *Chem. Phys. Lett.* **1987**, *133*, 189–192.
- [37] O. Mermut, D. C. Phillips, R. L. York, K. R. Mccrea, R. S. Ward, G. A. Somorjai, *J. Am. Chem. Soc.* **2006**, *128*, 3598–3607.
- [38] A. Peremans, A. Tadjeddine, *J. Chem. Phys.* **1995**, *103*, 7197–7203.
- [39] J. Wang, M. A. Even, X. Y. Chen, A. H. Schmaier, J. H. Waite, Z. Chen, *J. Am. Chem. Soc.* **2003**, *125*, 9914–9915.
- [40] M. Bonn, H. Ueba, M. Wolf, *J. Phys.* **2005**, *17*, S201–S220.
- [41] I. V. Stiopkin, H. D. Jayathilake, A. N. Bordenyuk, A. V. Bendetskii, *J. Am. Chem. Soc.* **2008**, *130*, 2271–2275.
- [42] P. B. Miranda, Y. R. Shen, *J. Phys. Chem. B* **1999**, *103*, 3292–3307.
- [43] M. L. Clarke, J. Wang, Z. Chen, *J. Phys. Chem. B* **2005**, *109*, 22027–22035.
- [44] J. Wang, S. H. Lee, Z. Chen, *J. Phys. Chem. B* **2008**, *112*, 2281–2290.
- [45] X. Y. Chen, J. Wang, A. P. Boughton, C. B. Kristalyn, Z. Chen, *J. Am. Chem. Soc.* **2007**, *129*, 1420–1427.
- [46] M. A. Even, J. Wang, Z. Chen, *Langmuir* **2008**, *24*, 5795–5801.
- [47] X. Y. Chen, A. P. Boughton, J. J. G. Tesmer, Z. Chen, *J. Am. Chem. Soc.* **2007**, *129*, 12658–12659.
- [48] F. Keilmann, *Vib. Spectrosc.* **2002**, *29*, 109–114.
- [49] B. Knoll, F. Keilmann, *Nature* **1999**, *399*, 134–137.
- [50] B. Knoll, F. Keilmann, *Appl. Phys. A* **1998**, *66*, 477–481.
- [51] I. Kopf, J. S. Samson, G. Wollny, C. Grunwald, E. Brundermann, M. Havenith, *J. Phys. Chem. C* **2007**, *111*, 8166–8171.
- [52] J. Steidtner, B. Pettinger, *Phys. Rev. Lett.* **2008**, *100*, 236101.
- [53] R. M. Stöckle, Y. D. Suh, V. Deckert, R. Zenobi, *Chem. Phys. Lett.* **2000**, *318*, 131–136.
- [54] R. B. Dyer, F. Gai, W. H. Woodruff, *Acc. Chem. Res.* **1998**, *31*, 709–716.
- [55] W. Uhmann, A. Becker, C. Taran, F. Siebert, *Appl. Spectrosc.* **1991**, *45*, 390–397.
- [56] I. Radu, M. Schleegeer, C. Bolwien, J. Heberle, *Photochem. Photobiol. Sci.* **2009**, *8*, 1517–1528.
- [57] F. Garczarek, K. Gerwert, *Nature* **2006**, *439*, 109–112.
- [58] T. Majerus, T. Kottke, W. Laan, K. Hellingwerf, J. Heberle, *ChemPhysChem* **2007**, *8*, 1787–1789.
- [59] A. Pfeifer, T. Majerus, K. Zikihara, D. Matsuoka, S. Tokutomi, J. Heberle, T. Kottke, *Biophys. J.* **2009**, *96*, 1462–1470.
- [60] M. T. Alexandre, D. C. Luhrs, I. van Stokkum, R. Hiller, M. L. Groot, J. T. Kennis, R. van Grondelle, *Biophys. J.* **2007**, *93*, 2118–2128.
- [61] V. Sivakumar, R. Wang, G. Hastings, *Biochemistry* **2005**, *44*, 1880–1893.
- [62] G. Hastings, K. M. Bandaranayake, E. Carrion, *Biophys. J.* **2008**, *94*, 4383–4392.
- [63] R. Efremov, V. I. Gordeliy, J. Heberle, G. Büldt, *Biophys. J.* **2006**, *91*, 1441–1451.
- [64] J. N. Moore, P. A. Hansen, R. M. Hochstrasser, *Proc. Natl. Acad. Sci. USA* **1988**, *85*, 5062–5066.
- [65] P. Hamm, M. Zurek, W. Mantele, M. Meyer, H. Scheer, W. Zinth, *Proc. Natl. Acad. Sci. USA* **1995**, *92*, 1826–1830.
- [66] R. W. Schoenlein, L. A. Peteanu, R. A. Mathies, C. V. Shank, *Science* **1991**, *254*, 412–415.
- [67] J. Herbst, K. Heyne, R. Diller, *Science* **2002**, *297*, 822–825.
- [68] J. J. van Thor, K. L. Ronayne, M. Towrie, *J. Am. Chem. Soc.* **2007**, *129*, 126–132.
- [69] C. Schumann, R. Gross, M. M. Wolf, R. Diller, N. Michael, T. Lamparter, *Biophys. J.* **2008**, *94*, 3189–3197.
- [70] L. J. van Wilderen, M. A. van der Horst, I. van Stokkum, K. J. Hellingwerf, R. van Grondelle, M. L. Groot, *Proc. Natl. Acad. Sci. USA* **2006**, *103*, 15050–15055.
- [71] A. L. Stelling, K. L. Ronayne, J. Nappa, P. J. Tonge, S. R. Meech, *J. Am. Chem. Soc.* **2007**, *129*, 15556–15564.
- [72] P. Hamm, M. H. Lim, R. M. Hochstrasser, *J. Phys. Chem. B* **1998**, *102*, 6123–6138.
- [73] M. C. Asplund, M. T. Zanni, R. M. Hochstrasser, *Proc. Natl. Acad. Sci. USA* **2000**, *97*, 8219–8224.
- [74] M. T. Zanni, R. M. Hochstrasser, *Curr. Opin. Struct. Biol.* **2001**, *11*, 516–522.
- [75] M. T. Zanni, S. Gnanakaran, J. Stenger, R. M. Hochstrasser, *J. Phys. Chem. B* **2001**, *105*, 6520–6535.
- [76] P. Hamm, M. Lim, W. F. DeGrado, R. M. Hochstrasser, *Proc. Natl. Acad. Sci. USA* **1999**, *96*, 2036–2041.
- [77] S. Woutersen, P. Hamm, *J. Phys. Chem. B* **2000**, *104*, 11316–11320.
- [78] M. T. Zanni, N. H. Ge, Y. S. Kim, R. M. Hochstrasser, *Proc. Natl. Acad. Sci. USA* **2001**, *98*, 11265–11270.

- [79] N. Demirdöven, C. M. Cheatum, H. S. Chung, M. Khalil, J. Knoester, A. Tokmakoff, *J. Am. Chem. Soc.* **2004**, *126*, 7981–7990.
- [80] H. Maekawa, F. Formaggio, C. Toniolo, N. H. Ge, *J. Am. Chem. Soc.* **2008**, *130*, 6556–6566.
- [81] H. Maekawa, C. Toniolo, Q. B. Broxterman, N. H. Ge, *J. Phys. Chem. B* **2007**, *111*, 3222–3235.
- [82] L. P. Deflores, Z. Ganim, R. A. Nicodemus, A. Tokmakoff, *J. Am. Chem. Soc.* **2009**, *131*, 3385–3391.
- [83] C. Fang, J. Wang, Y. S. Kim, A. K. Charnley, W. Barber-Armstrong, A. B. Smith, S. M. Decatur, R. M. Hochstrasser, *J. Phys. Chem. B* **2004**, *108*, 10415–10427.
- [84] P. Mukherjee, I. Kass, I. T. Arkin, M. T. Zanni, *Proc. Natl. Acad. Sci. USA* **2006**, *103*, 3528–3533.
- [85] Y. S. Kim, L. Liu, P. H. Axelsen, R. M. Hochstrasser, *Proc. Natl. Acad. Sci. USA* **2008**, *105*, 7720–7725.
- [86] D. B. Strasfeld, Y. L. Ling, S. H. Shim, M. T. Zanni, *J. Am. Chem. Soc.* **2008**, *130*, 6698–6699.
- [87] S. H. Shim, R. Gupta, Y. L. Ling, D. B. Strasfeld, D. P. Raleigh, M. T. Zanni, *Proc. Natl. Acad. Sci. USA* **2009**, *106*, 6614–6619.
- [88] J. Manor, P. Mukherjee, Y. S. Lin, H. Leonov, J. L. Skinner, M. T. Zanni, I. T. Arkin, *Structure* **2009**, *17*, 247–254.
- [89] O. Bieri, J. Wirz, B. Hellrung, M. Schutkowski, M. Drewello, T. Kiefhaber, *Proc. Natl. Acad. Sci. USA* **1999**, *96*, 9597–9601.
- [90] C. Kolano, J. Helbing, M. Kozinski, W. Sander, P. Hamm, *Nature* **2006**, *444*, 469–472.
- [91] H. S. Chung, Z. Ganim, K. C. Jones, A. Tokmakoff, *Proc. Natl. Acad. Sci. USA* **2007**, *104*, 14237–14242.
- [92] J. Bredenbeck, J. Helbing, K. Nienhaus, G. U. Nienhaus, P. Hamm, *Proc. Natl. Acad. Sci. USA* **2007**, *104*, 14243–14248.
- [93] H. Ishikawa, K. Kwak, J. K. Chung, S. Kim, M. D. Fayer, *Proc. Natl. Acad. Sci. USA* **2008**, *105*, 8619–8624.
- [94] E. R. Andresen, P. Hamm, *J. Phys. Chem. B* **2009**, *113*, 6520–6527.
- [95] A. Ghosh, M. Smits, J. Bredenbeck, N. Dijkhuizen, M. Bonn, *Rev. Sci. Instrum.* **2008**, *79*, 093907.
- [96] J. Bredenbeck, A. Ghosh, M. Smits, M. Bonn, *J. Am. Chem. Soc.* **2008**, *130*, 2152–2153.
- [97] J. F. Cahoon, K. R. Sawyer, J. P. Schlegel, C. B. Harris, *Science* **2008**, *319*, 1820–1823.